Available online at www.CivileJournal.org

Civil Engineering Journal

(E-ISSN: 2476-3055; ISSN: 2676-6957)

Vol. 9, No. 03, March, 2023

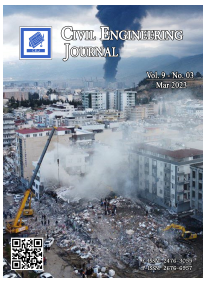

Finite Element Analysis of Two Nearby Interfering Strip Footings Embedded in Saturated Cohesive Soils

Mo'men Ayasrah [1*], Mohammed Y. Fattah [2]

[1] *Department of Civil Engineering, Faculty of Engineering, Al Al-Bayt University, Mafraq 25113, Jordan.*

[2] *Professor, Department of Civil Engineering, University of Technology, Baghdad, Iraq.*

Received 23 December 2022; Revised 09 February 2023; Accepted 22 February 2023; Published 01 March 2023

Abstract

The issue of interaction between nearby footings is of paramount practical significance. The interference effect should be taken into account since the footing may really be separated from or bounded by other footings on one or both sides. In this regard, this paper studies the effect of two nearby interfering strip footings embedded in saturated cohesive soils, which will help to provide a better understanding of the impact of footing depth on the interference effect. A numerical study is carried out using the finite element program (Midas GTS-NX), and the behavior of closely placed strip footings embedded in the saturated cohesive soils is investigated under the influence of different factors such as the spacing between footings, the depth of footings, soil undrained shear strength, and the groundwater table. It was concluded that the soil cohesion and the footing depth ratio have a notable influence on the interference of closely spaced footings. For all cohesion values, it has been observed that the spacing needed for interference to vanish decreases with an increase in the depth of the footing and water table. In addition, as the S/B ratio increases, the ultimate bearing capacity (UBC) of interfering footings decreases until it reaches the same value as an isolated footing at greater spacing. The UBC is approximately 10% higher at S/B = 1 compared to the isolated footing. However, at S/B = 1, the UBC of two footings achieves a value equal to that of an isolated footing and does not change when the S/B ratio increases. With increasing footing depth, there is an increase in UBC. Finally, the highest values of ξ were obtained in all cases when Cu = 40 kPa. This indicates that the interaction between footings is greater when the soil is softer.

Keywords: Finite Elements; Strip Footings; Interference; Saturated Clay; Bearing Capacity.

1. Introduction

Land availability is drastically decreasing worldwide as a result of rapid urbanization and population growth. Due to this, many structures are frequently constructed close to one another. Therefore, the interference effect should be taken into account since the footing may really be separated from or bounded by other footings on one or both sides. In addition, settlement of the foundation is a crucial design factor under working-load circumstances. The soil experiences stress-strain states that are neither linearly elastic nor perfectly plastic as a result of well-designed foundations. Settlements frequently favour footing construction on sandy soil and soft clay over bearing capacity. Therefore, settlement predictions are essential for the design of shallow foundations. When evaluating isolated footing capacity while taking allowable settlement requirements into account, the influence of neighboring footings is frequently overlooked. In this regard, numerous experiments and numerical analyses have been carried out to ascertain the interference impact of two nearby shallow foundations [1–6].

* Corresponding author: ayasrahmomen@aabu.edu.jo

http://dx.doi.org/10.28991/CEJ-2023-09-03-017

Kumar & Saran (2003) [7] proposed an analytical approach to defining the pressure related to a particular settlement for closely spaced strip footings on reinforced sand. Many laboratory-scaled model tests were performed on a dry, medium-density, reinforced Ennore sand bed to investigate the effect of interference between two neighboring surface strip footings. In the southern region of India, Ennore sand can be found in abundance. As a result, it was determined that the investigation of footing interference on Ennore sand was important. The type of strip footings made using mild steel were intended to behave like rigid footings, and the roughness of the base was achieved by gluing sand paper to the ground beneath the footings. In addition, to reinforce the soil, a single layer of uniaxial geogrid was used.

A number of model tests were conducted by Ghosh & Kumar (2009) [8] to investigate the interference effect of two nearby strip footings on dry, reinforced Ennore sand substrates. The foundation bed was reinforced using a single layer of uniaxial geogrid. The results of the experimental study showed that with an increase in D/B, where D and B are the reinforcement depth and the footing width, respectively, the bearing capacity of single footings on the reinforced soil decreases. In addition, increases in footing width are observed to result in a reduction in the bearing capacity factor resulting from the soil's unit weight. The interfering footing settlement behavior was noted to show the same pattern as the bearing capacity. The results were obtained by efficiency factors (ξ_{γ}, ξ_{δ}) and their difference was found due to changes in spacing. The results of experimental studies were generally found to be in good accord with the experimental and theoretical results available in the literature.

An attempt was made by Ghosh (2013) [9] to simulate the response of the seismic system of two embedded rectangular or square footings located in nearby spacing on a layered soil deposit resting on strong bed rock by using the finite difference code FLAC3D. Without exceeding the ultimate bearing capacity under static conditions, each footing conveys an equivalent static working load. It was presumed that the soil would obey the non-linear Mohr-Coulomb failure criteria. Based on their study, the results given in the cases of the horizontal acceleration response on the top surface of the footing, the settlement, and ultimate bearing capacity under both conditions; static and seismic reflect the difference in the clear distance between footings and the stresses generated at the base of each footing due to seismic excitation. It is found that the settlement of two nearby footings due to seismic conditions is higher than that of a single footing.

Using finite element analysis, Nainegali et al. (2013) [10] investigated the interaction of two rigid strip footings that are closely spaced and rest on a homogeneous soil bed in order to determine their settlement behavior and ultimate bearing capacity under inclined loading. In their study, the soil was modeled using the Mohr-Coulomb failure criterion, and many parametric studies, such as the clear distance between the footing and the inclination angle, were carried out. The results indicated that the settlement and bearing capacity for interacting footings were greater than for single footings when the distance between the footings was decreased and there was no effect from the inclined load. In the same line, the bearing capacity of two adjacent strip footings on the sand was examined by Shokoohi et al. (2019) [11] using finite element and limited equilibrium methods. The results of the ratio of the bearing capacity show that both approaches are in line with the data that is accessible in the literature.

Acharyya et al. (2020) [12] used Plaxis 3D to conduct a series of finite element calculations to examine the bearing capacity of a square footing positioned on the slope's crest. For the direct prediction of bearing capacity, an ideal artificial neural network (ANN) architecture was also constructed. It was found that the bearing capacity value is significantly influenced by the soil's shear strength parameters, the width of the footing, the depth of embedment, and the slope inclination.

Anaswara & Shivashankar (2019) [13] conducted parametric experiments for two footings by altering the distance between the footings and the footing width. In the first instance, both footings were simultaneously loaded until they failed. In the second case, one of the existing foundation footings was loaded with half of the evaluated failure load for a single footing, and a neighboring footing was loaded all the way to failure. The effect of interference was observed to be particularly significant in terms of the settlement. The effect of shear keys placed beneath the footings at different locations beneath the footing and the interference of such footings were also studied in the case of stiff clay. It was discovered that the presence of shear keys has a significant effect on interference between footings when compared to not having them, particularly in reducing foundation tilt.

On the other hand, Boufarh et al. (2020) [14] conducted a numerical finite element analysis to study the interference influence on the seismic bearing capacity of nearby spaced rigid strip footings for a varying range of footing spacings, angles of friction, and the factor of the horizontal acceleration. The findings showed that an increase in seismic acceleration reduces efficiency gains because the failure zone of footings interferes with footing performance. Moreover, Meraz et al. (2022) [15] evaluated the effects of a surrounding footing with a variable distance in soft soil situations by using the finite element analysis program PLAXIS. They noticed a significant capacity difference with different numbers of footings and distances. As a result, taking this capacity variation into account can lead to a safer design.

From the ongoing discussion of footing performance in close proximity, the reported results are in relation to surface footings or the surcharge at the base of the footing. However, the impact of the interference of footing state is seldom

acknowledged. In addition, in practice, it is rare to find footings that are laid level with the ground. Therefore, the footings were laid down in an embedded state on the soil medium. In this paper, the effect of two nearby interfering strip footings embedded in saturated cohesive soils was studied to provide a better understanding of the impact of footing depth on the interference effect.

The remainder of this paper is organized as follows. Section 2 presents the details of the problem statement. In Section 3, the finite element method, construction stages, and bearing capacity ratio definition are explained. The computational results are presented and analyzed in Section 4. Finally, conclusions are drawn in Section 5. In addition, the research flowchart is shown in Figure 1.

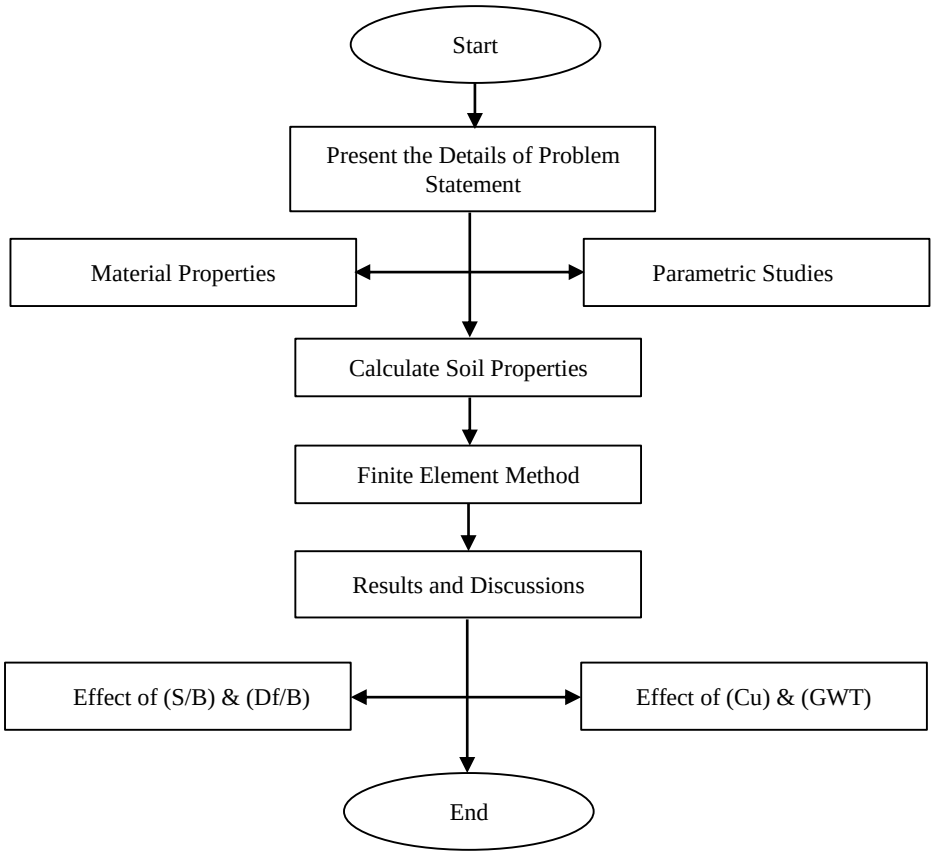

Figure 1. Flowchart of the present study

2. Problem Statement Considered in This Study

In this work, two strip footings are taken to explore the influence of their interference on the bearing capacity of saturated cohesive soils. The strip footings have a width (B) of 2.0 m and a thickness (H) of 0.3m. In addition, the spacing between footings (S), depth of footings (Df), undrained shear strength of the clay (Cu), and ground water table (GWT) are changed. Therefore, a finite element analysis is established for each case. The parametric studies that are considered in this study are presented in Table 1.

Table 1. Soil properties, footings, and parametric studies

Parameters	γ, kN/m^3	Cu, kN/m^2	E, kN/m^2	υ
Clay	18	40	40000	0.3
		60	60000	
		100	100000	
Footings	24		25×10^6	0.2
Range of varying parameters				
Df/B	0.25	0.5	1	1.5
S/B	0.5	1	2	4
GWT	0	2	4	
Cu	40	60	100	

3. Numerical Modeling

3.1. Finite Element Method

In this research, a numerical study is carried out using the finite element program (Midas GTS-NX), and the behavior of closely placed strip footings embedded in the saturated cohesive soils is investigated. The mesh dimensions of the soil domain in the horizontal are 33 B, while 12 B is in the vertical direction; B is the width of the strip footings. These dimensions were carried out and determined based on a sensitivity study. In addition, a relatively fine mesh was simulated near the strip footings and become coarser mesh further from outside these zones. In the case of defining the boundaries condition, the bottom surface was assumed to be hinged to prevent the horizontal and vertical movements, while, a roller was applied in the left and right sides of the soil to allow vertical movement only. The plane strain mesh and geometrical boundaries are shown in Figure 2. It is worth mentioning that the load is applied on each footing as uniformly pressure. In this model, the mesh consists of 6706 nodes and 6591 elements. To be noticed, the numbers of elements and nodes are varied slightly in each model owing to the auto mesh generation technique in the Midas GTS-NX program. In addition, the side boundaries are exclusively fixed in the horizontal direction, and the bottom end is connected to fixed supports (no displacements are permitted).

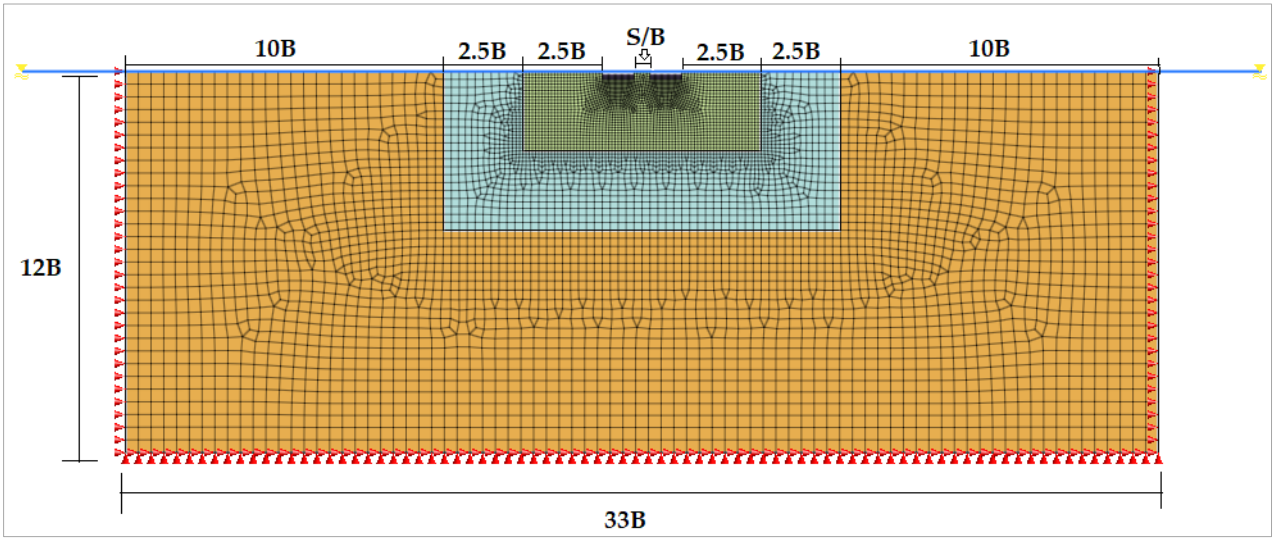

Figure 2. The finite element mesh of the problem and boundary conditions

To introduce the soil and footings parameters', the Mohr-Columb constitutive model was utilized to simulate the soil materials due to its simplicity and accuracy [16] and it is widely used in finite element analyses of geotechnical engineering among which the undrained bearing capacity issues [17-22]. On the other hand, the footings were simulated as the linear elastic model. The required parameters for soil and footings are presented in Table 1.

In the present work, all the models are simulated using Midas Gts nx employing the undrained parameters. Therefore, the friction angle (φ) and dilation angle (ψ) equal to zero were prescribed for undrained condition. In addition, the undrained modulus of clays (E_u) is calculated using the following equation which is proposed by Ameratunga et al. (2016) [23]:

$$E = (100 \text{-} 1000)\ C_u \quad (1)$$

It is worthy to add that the undrained Poisson's ratio for soil undrained is utilized with 0.495 rather than 0.50 to prevent any numerical problems. Therefore, the Mohr-Coulomb model is used to simulate the undrained soil condition, and the drainage parameter is taken with the third option; Undrained (Effective stiffness/Undrained strength) in Midas GTS-NX. Furthermore, the coefficient of lateral earth pressure at rest (k_0) has been calculated as 1.00, according to the following equation:

$$k_0 = \upsilon/(1+\upsilon) \quad (2)$$

where, υ is undrained Poisson's ratio.

3.2. Construction Stages

The same soil properties and footing elements listed in Table 1, were used in the two-dimensional model. The stages can be stated as follow:

1- Initial Stage (I.S): this stage starts with generating the initial stress of the soil before strip footings implementation. In addition, activated the boundary conditions.

2- Stage 1 (S1): the left and right footings are activated. Also, at this stage, the displacements were reset to zero in order to start to account for bearing capacity due to the applied loads only.

3- Stage 2 (S2): this stage includes applying the loads to footings using forty incremental loading steps to simulate load-settlement behavior.

The first state of stress is crucial for the analysis of geotechnical problems, so before applying the loads to footings, the soil is examined for its initial state of stress using a geostatic stage where the gravity load is applied.

3.3. Definition of Bearing Capacity Ratio (ξ)

The evaluated ultimate bearing capacity UBC is represented in terms of non-dimensional efficiency factors for UBC: ξL/ξR (Left/Right):

$$\xi_L/\xi_R = \frac{UBC\ of\ left/right\ footing\ in\ presence\ of\ right/left\ footing}{UBC\ of\ identical\ isolated\ footing} \quad (3)$$

4. Results and Discussions

4.1. Effect of the Spacing Ratio (S/B)

Figure 3 shows the load-settlement curves for footings (Left and right) in a soil of undrained shear strength, cu = 40 kPa with different depths and water table level in case the spacing ratio between the footings (S/B) is 1. The results of other footings with different spacing ratios are listed in Table 2.

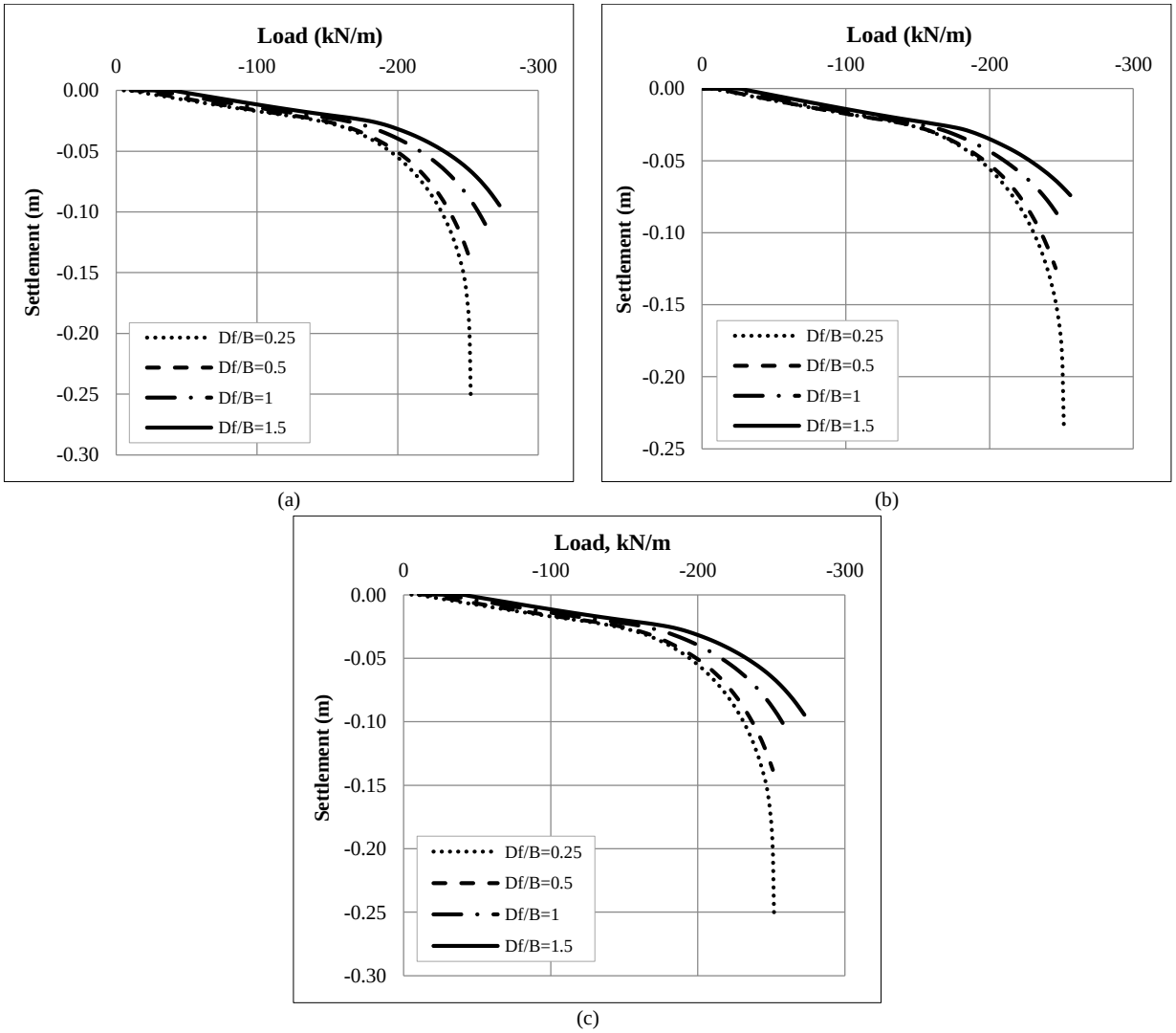

Figure 3. Load settlement curve for Cu = 40 kPa for left and right footing with S/B = 0.5 and a) GWT = 0, GWT = 2 m and c) GWT = 4 m

Table 2. The ultimate bearing capacity of footings based on the load settlement curves.

Cu kPa	GWT m	S/B	D_f/B	q_u kPa	Cu kPa	GWT m	S/B	D_f/B	q_u kPa	Cu kPa	GWT m	S/B	D_f/B	q_u kPa
40	0	1	0.25	245	60	0	1	0.25	340	100	0	1	0.25	570
			0.5	260				0.5	345				0.5	580
			1	280				1	350				1	588
			1.5	284				1.5	355				1.5	593
		2	0.25	230			2	0.25	335			2	0.25	560
			0.5	240				0.5	338				0.5	570
			1	250				1	340				1	580
			1.5	280				1.5	345				1.5	587
		4	0.25	227			4	0.25	330			4	0.25	555
			0.5	235				0.5	335				0.5	560
			1	245				1	338				1	575
			1.5	270				1.5	342				1.5	580
	2	1	0.25	250		2	1	0.25	360		2	1	0.25	580
			0.5	265				0.5	370				0.5	585
			1	290				1	375				1	592
			1.5	295				1.5	380				1.5	597
		2	0.25	245			2	0.25	355			2	0.25	565
			0.5	250				0.5	360				0.5	575
			1	255				1	365				1	585
			1.5	285				1.5	375				1.5	593
		4	0.25	230			4	0.25	350			4	0.25	560
			0.5	245				0.5	355				0.5	565
			1	253				1	360				1	580
			1.5	275				1.5	365				1.5	585
	4	1	0.25	255		4	1	0.25	380		4	1	0.25	585
			0.5	270				0.5	385				0.5	590
			1	295				1	390				1	595
			1.5	300				1.5	400				1.5	600
		2	0.25	250			2	0.25	370			2	0.25	570
			0.5	260				0.5	375				0.5	580
			1	275				1	383				1	590
			1.5	290				1.5	390				1.5	595
		4	0.25	240			4	0.25	360			4	0.25	565
			0.5	250				0.5	370				0.5	570
			1	265				1	378				1	585
			1.5	285				1.5	385				1.5	590

The ultimate bearing capacity of the footing is considered to be the load that causes continuous settlement divided by the footing area. It is noticed that the curves acquired from the left and right footings are seen to be exactly identical. It is concluded from Table 2 that the UBC of interfering footings decreases as the S/B ratio increases and attains the value of an isolated footing at greater spacing. In addition, the UBC is approximately 10% higher at S/B = 1 compared to the isolated footing, this is due to the stress zones overlapping individual footing when put close to each other. As shown in Figure 2, it can be seen that the behavior of the load settlement curve is the same in all cases. In addition, an analogous form of difference is noticed for the settlements at working load. Moreover, when the footings are positioned with S/B = 2, the settlement increases by 48%, and as the S/B ratio increases, the percentage increase in the settlement reduces.

However, at S/B = 1, the UBC of two footings achieves a value equal to that of an isolated footing and does not change when the S/B ratio increases. In addition, there is an increase in UBC with the increased depth of footings. For example, when cu = 40 kPa, S/B = 1, the UBC increases by 6 and 14%, respectively, as the depth of footings Df/B increases from 0.25 to 0.5 and a, respectively.

4.2. Effect of the Undrained Shear Strength of the Clay (Cu)

Figures 4 to 9 present the variation of bearing capacity ratio ξL/ξR with cu or different values of Df//B and water table level. Table 3 summarizes the values of ξ for different cases.

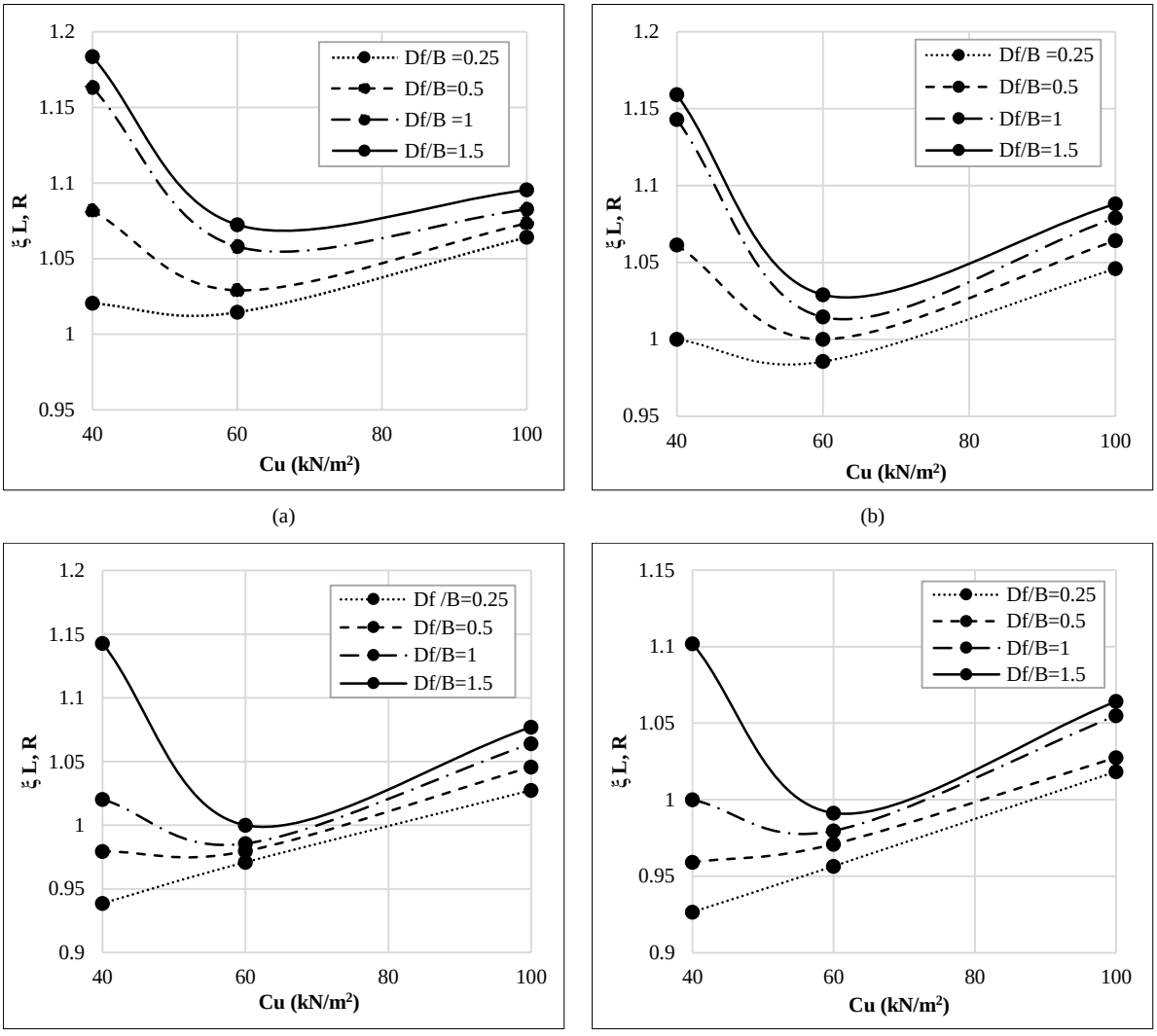

Figure 4. Variation of $\xi_{L,R}$ with Cu for different Df/B of the footing and GWT = 0 for (a) S/B=0.5 (b) S/B=1, (c) S/B=2, and (d) S/B=4

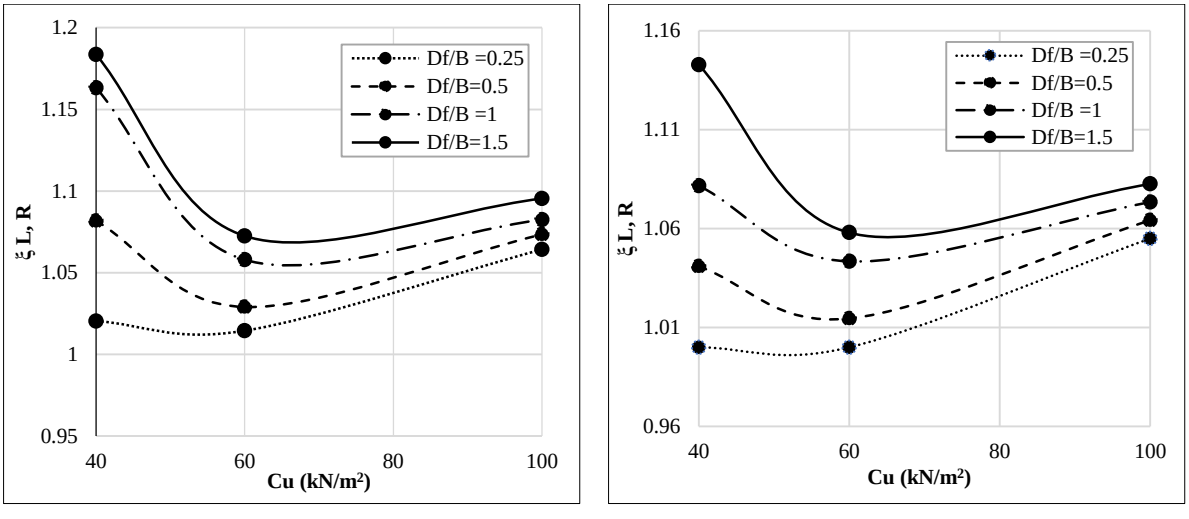

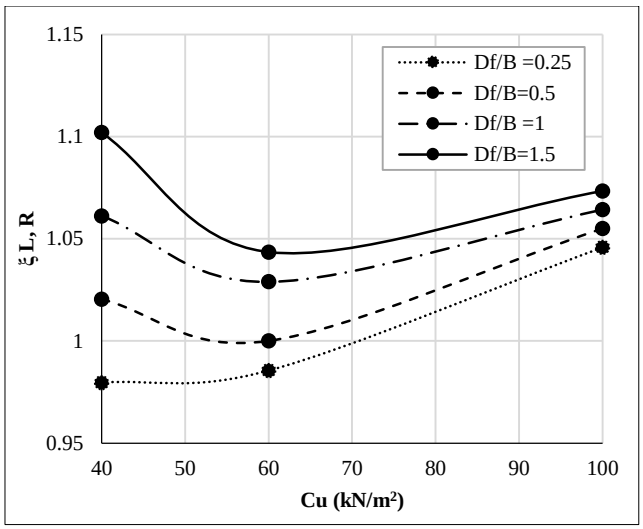

(c)

Figure 5. Variation of $\xi_{L,R}$ with Cu for different depth of the footing with S/B = 0.5 for (a) GWT =0 (b) GWT = 2, and (c) GWT = 4 m

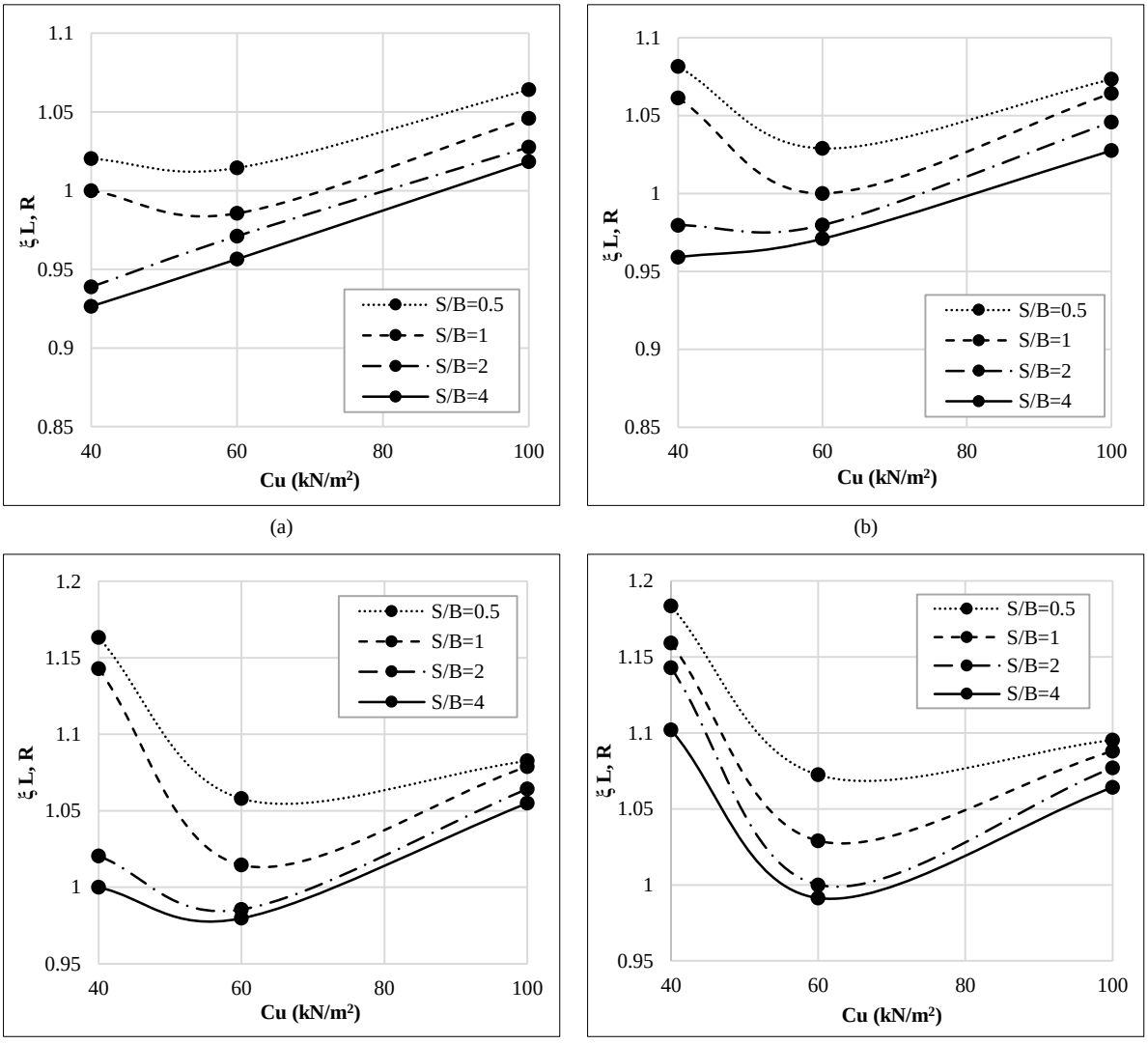

(a) (b)

(c) (d)

Figure 6. Variation of $\xi_{L,R}$ with Cu for different S/B of the footing and GWT= 0 for (a) Df/B = 0.25, (b) Df/B = 0.5, (c) Df/B =1, and (d) Df/B = 1.5

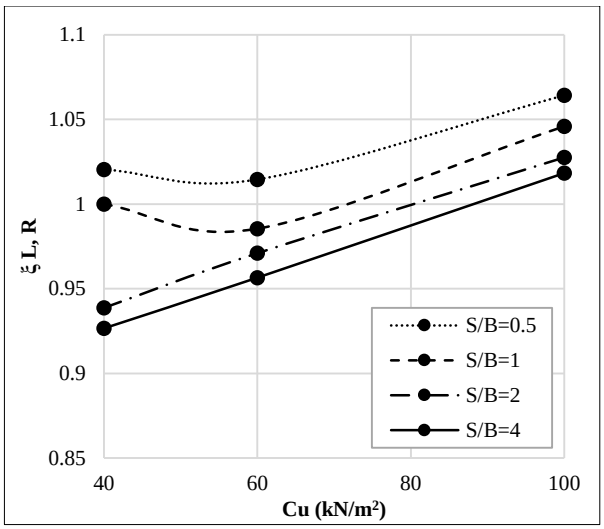

(a)

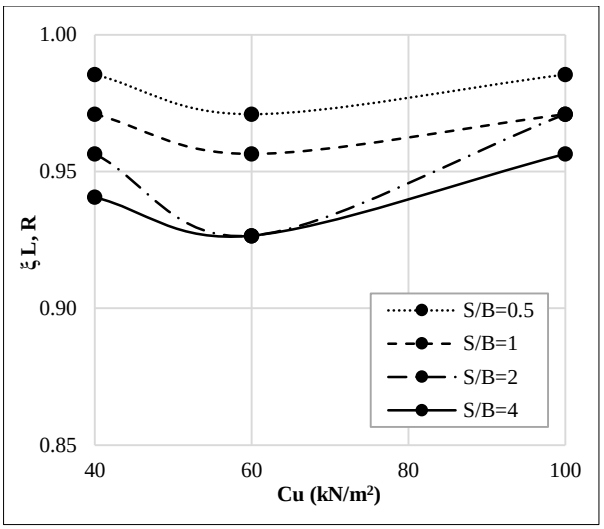

(b)

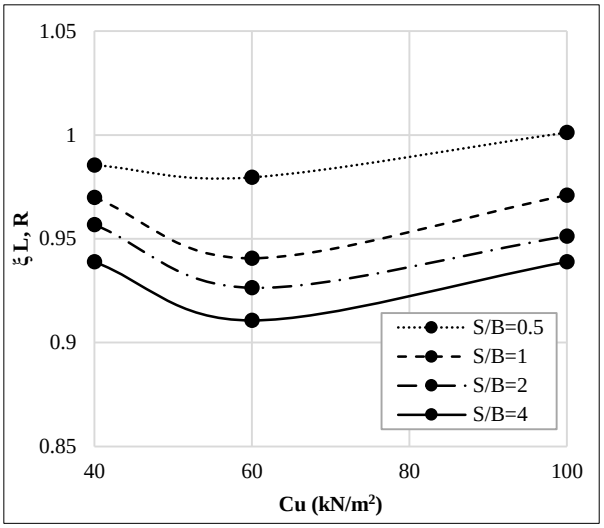

(c)

Figure 7. Variation of $\xi_{L,R}$ with Cu for different S/B of the footing and Df/B =0.25 for (a) GWT = 0, (b) GWT = 2 m, and (c) GWT = 4 m

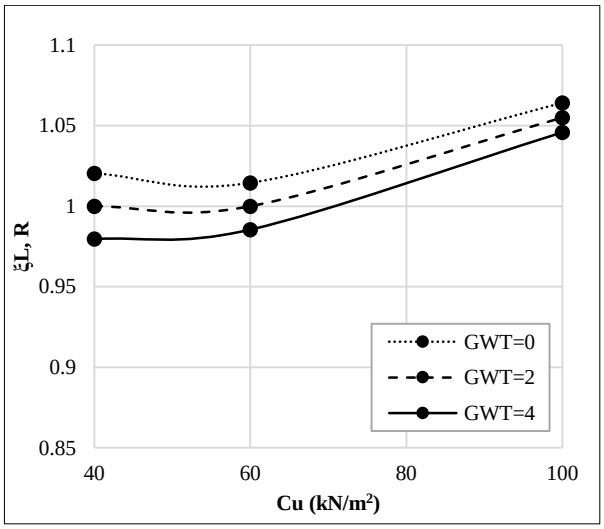

(a)

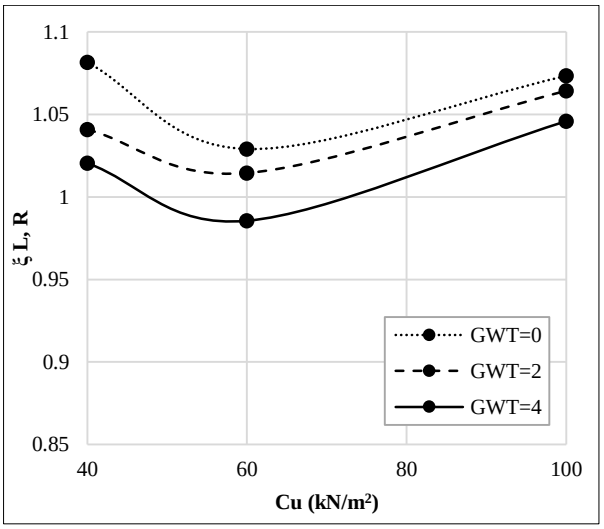

(b)

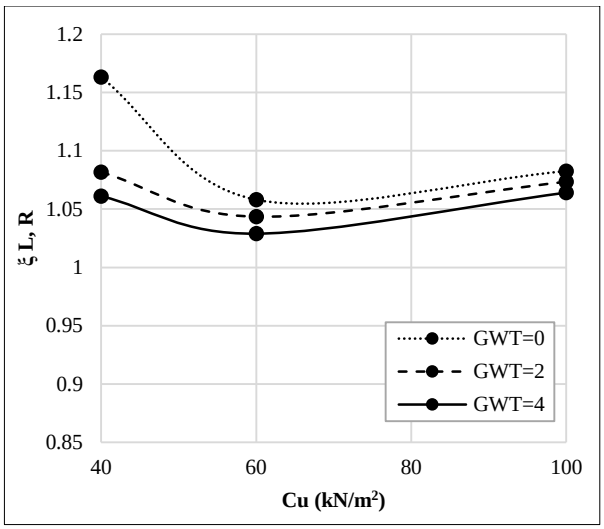

(c)

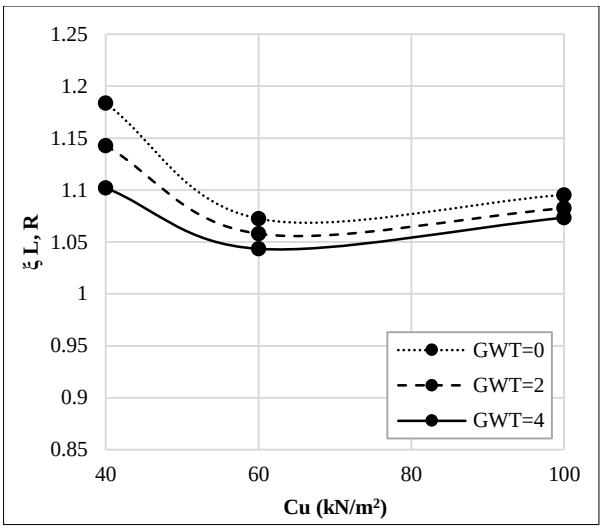

(d)

Figure 8. Variation of $\xi_{L,R}$ with Cu for different GWT and S/B =0.5 for (a) Df/B = 0.25, (b) Df/B = 0.5, (c) Df/B = 1 and (d) Df/B = 1.5

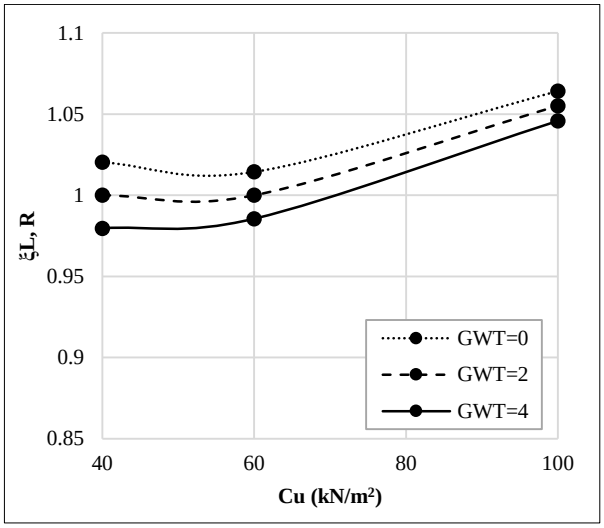

(a)

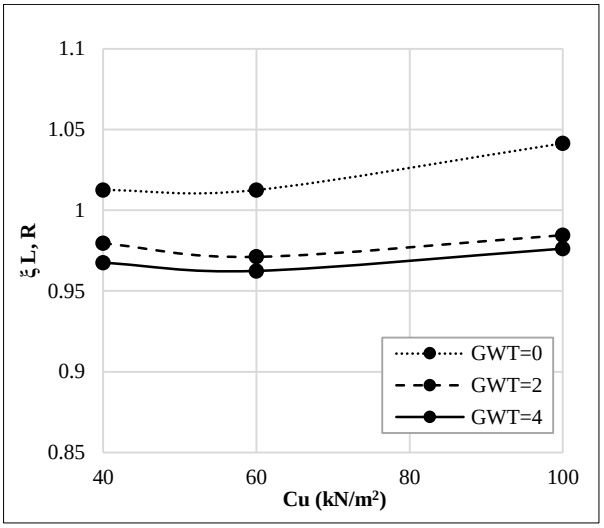

(b)

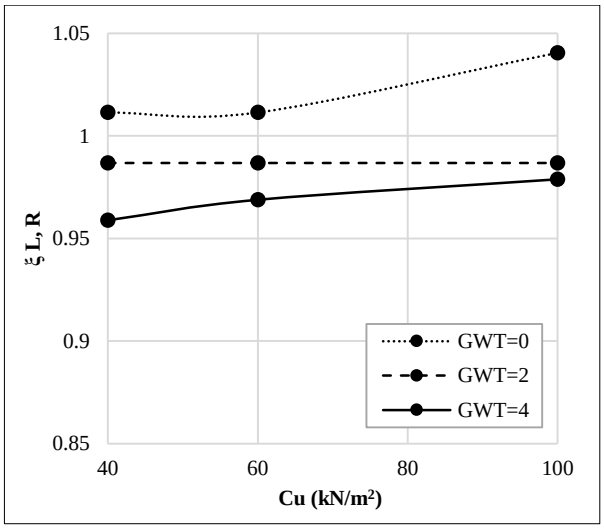

(c)

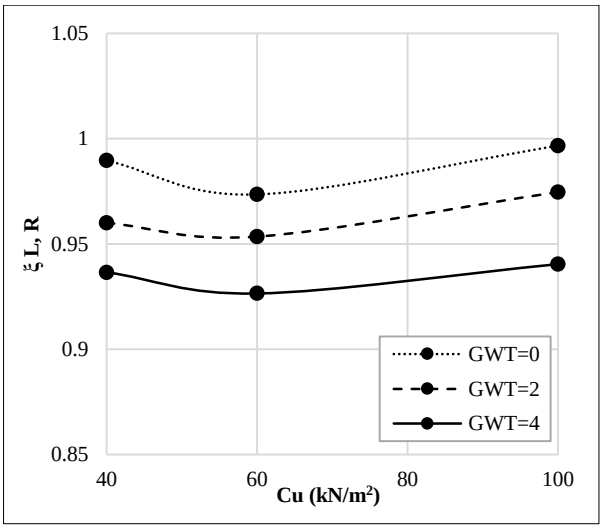

(d)

Figure 9. Variation of $\xi_{L,R}$ with Cu for different GWT and Df/B =0.25 for (a) S/B = 0.5, (b) S/B = 1, (c) S/B =2 and (d) S/B = 4

Table 3. Values of ξ for different Cu, GWT, S/B and Df/BL values, cu = 60 kPa

Cu kPa	GWT m	S/B	D_f/B	ξ	Cu kPa	GWT (m)	S/B	D_f/B	ξ	Cu kPa	GWT (m)	S/B	D_f/B	ξ
40	0	1	0.25	1	60	0	1	0.25	0.99	100	0	1	0.25	1.05
			0.5	1.06				0.5	1.00				0.5	1.06
			1	1.14				1	1.01				1	1.08
			1.5	1.16				1.5	1.03				1.5	1.09
		2	0.25	0.94			2	0.25	0.97			2	0.25	1.03
			0.5	0.98				0.5	0.98				0.5	1.05
			1	1.02				1	0.99				1	1.06
			1.5	1.14				1.5	1.00				1.5	1.08
		4	0.25	0.93			4	0.25	0.96			4	0.25	1.02
			0.5	0.96				0.5	0.97				0.5	1.03
			1	1.00				1	0.98				1	1.06
			1.5	1.10				1.5	0.99				1.5	1.06
	2	1	0.25	1.02		2	1	0.25	1.04		2	1	0.25	1.06
			0.5	1.08				0.5	1.07				0.5	1.07
			1	1.18				1	1.09				1	1.09
			1.5	1.20				1.5	1.10				1.5	1.10
		2	0.25	1.00			2	0.25	1.03			2	0.25	1.04
			0.5	1.02				0.5	1.04				0.5	1.06
			1	1.04				1	1.06				1	1.07
			1.5	1.16				1.5	1.09				1.5	1.09
		4	0.25	0.94			4	0.25	1.01			4	0.25	1.03
			0.5	1.00				0.5	1.03				0.5	1.04
			1	1.03				1	1.04				1	1.06
			1.5	1.12				1.5	1.06				1.5	1.07
	4	1	0.25	1.04		4	1	0.25	1.10		4	1	0.25	1.07
			0.5	1.10				0.5	1.12				0.5	1.08
			1	1.20				1	1.13				1	1.09
			1.5	1.22				1.5	1.16				1.5	1.10
		2	0.25	1.02			2	0.25	1.07			2	0.25	1.05
			0.5	1.06				0.5	1.09				0.5	1.06
			1	1.12				1	1.11				1	1.08
			1.5	1.18				1.5	1.13				1.5	1.09
		4	0.25	0.98			4	0.25	1.04			4	0.25	1.04
			0.5	1.02				0.5	1.07				0.5	1.05
			1	1.08				1	1.10				1	1.07
			1.5	1.16				1.5	1.12				1.5	1.08

It can be noticed that the bearing capacity ratio ξ increases with footing depth while decreasing with increasing of water table depth. In all cases, the largest values of ξ were obtained when cu = 40 kPa. This indicates that the interaction between footings is greater when the soil is softer.

The UBC of the interfering footing is observed to fall by 5–10% at S/B = 1 and 2, respectively, while the bearing capacity value of the at-surface footing is still equal to that of the isolated footing, indicating negligible or no influence of interference on the bearing capacity. However, the interference has a noticeable impact on the settlement.

When the distance between the foundations is greater than 1, the effect of the increase in the depth of the foundation overcomes the effect of the decrease in the bearing capacity resulting from the increase in the distance between the foundations.

4.3. Effect of the Depth of Footings Ratio (Df/B)

Figures 10 to 15 display the variation of $\xi_{L,R}$ with spacing ratio S/B for different values of footing depth and water table depth.

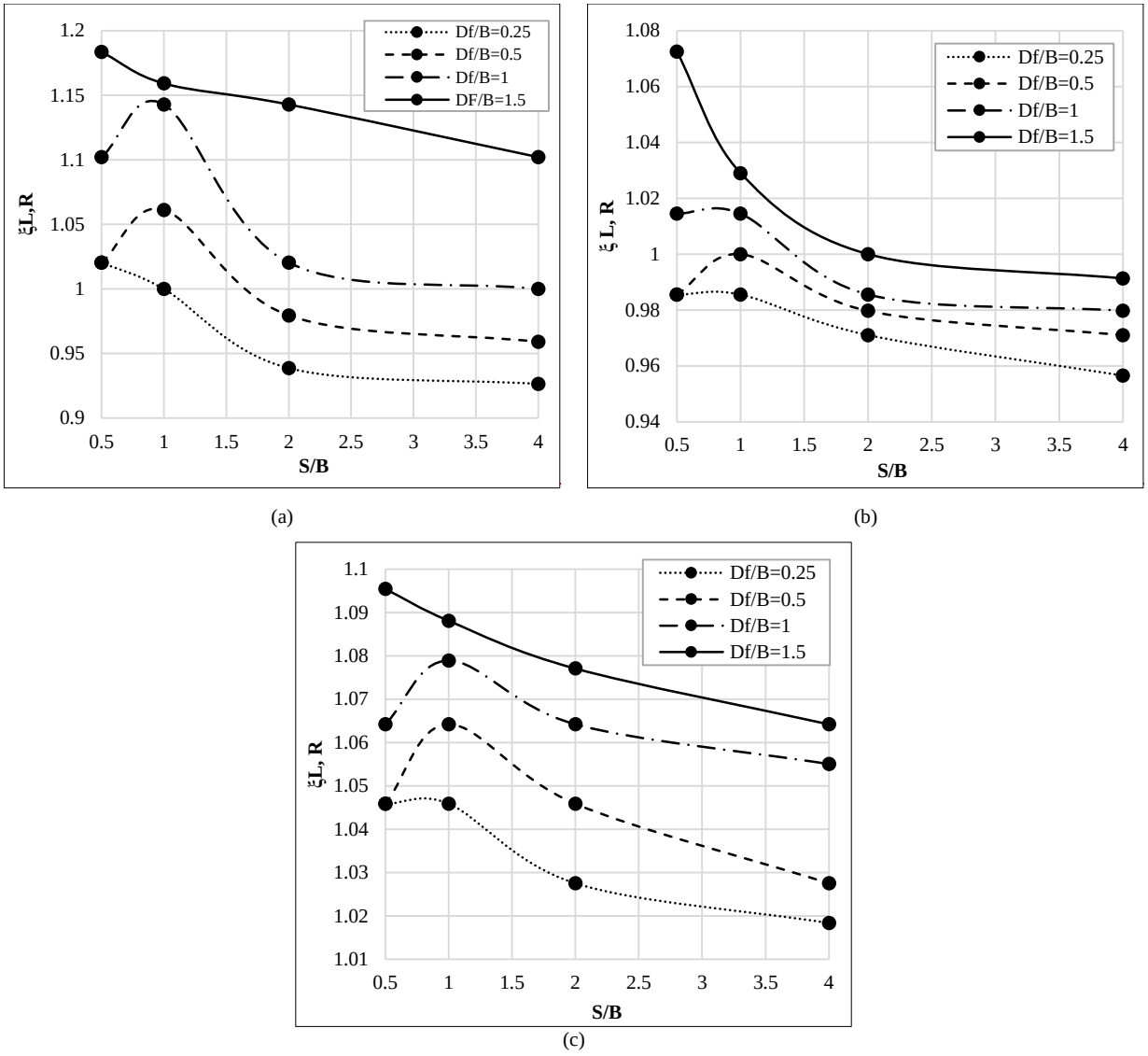

Figure 10. Variation of $\xi_{L,R}$ with S/B for different Df/B and GWT =0 for (a) Cu= 40 kPa, (b) Cu= 60 kPa, and (c) Cu = 100 kPa

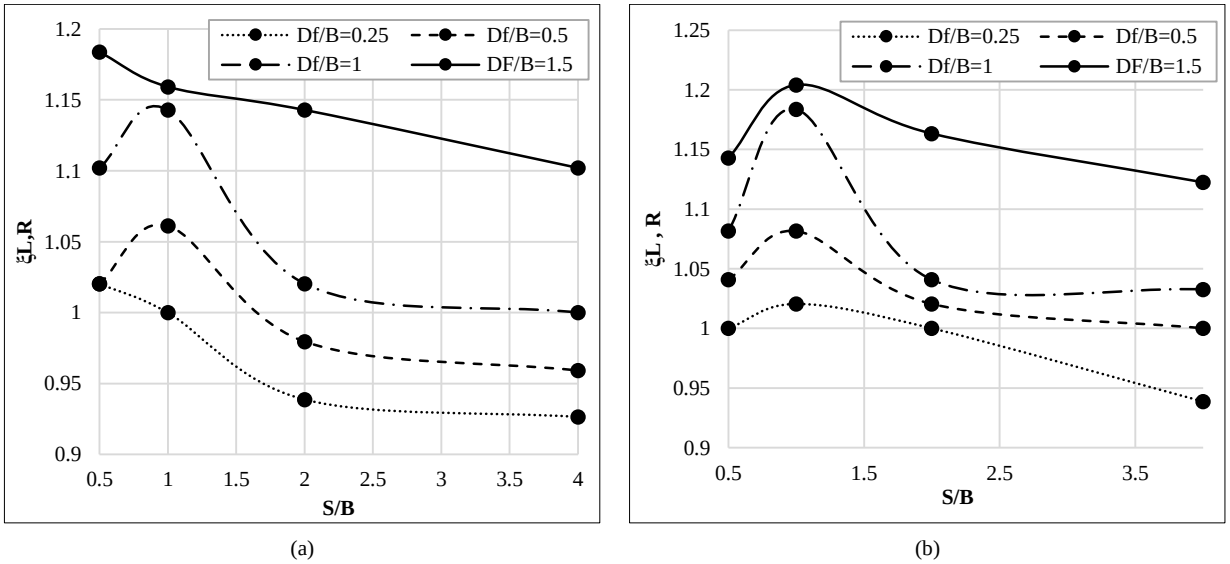

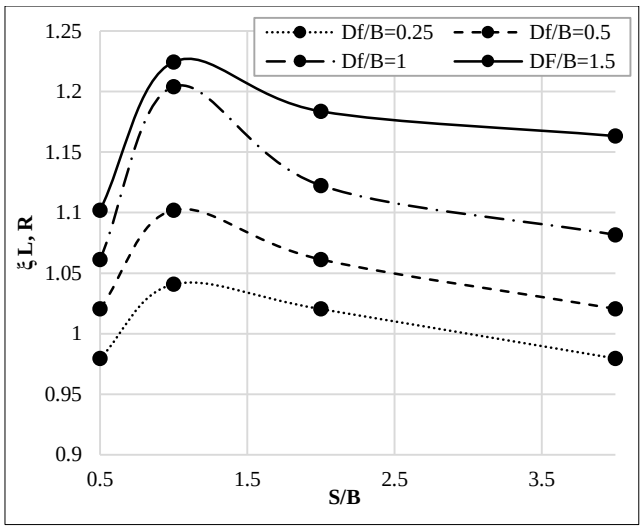

(c)

Figure 11. Variation of $\xi_{L,R}$ with S/B for different Df/B and Cu=40 kPa for (a) GWT=0, (b) GWT =2m, and (c) GWT=4 m

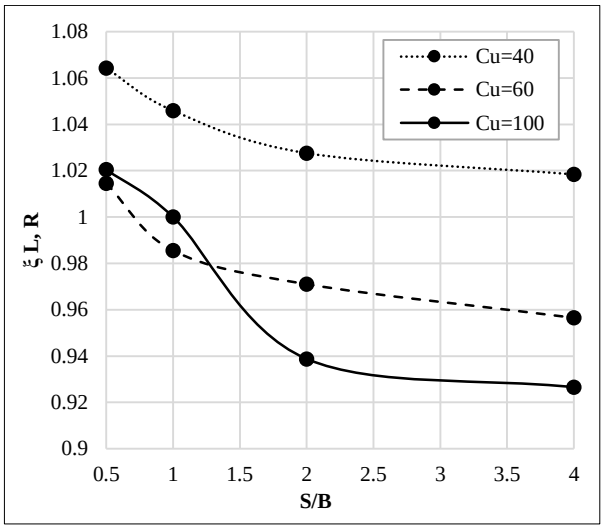

(a)

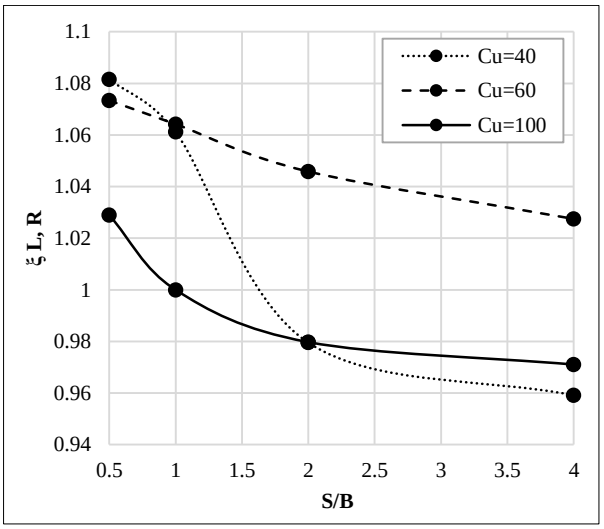

(b)

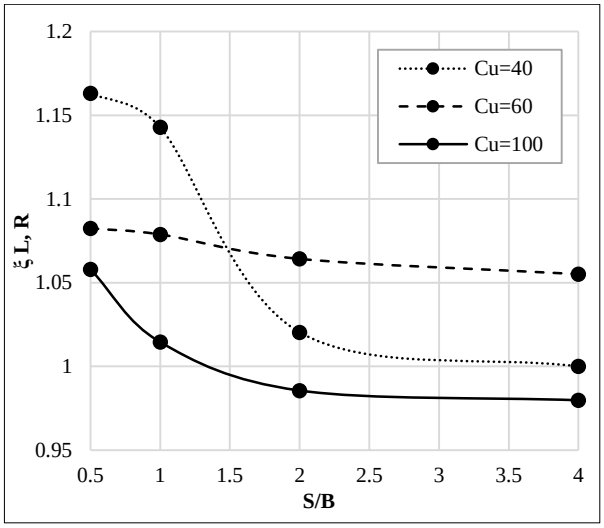

(c)

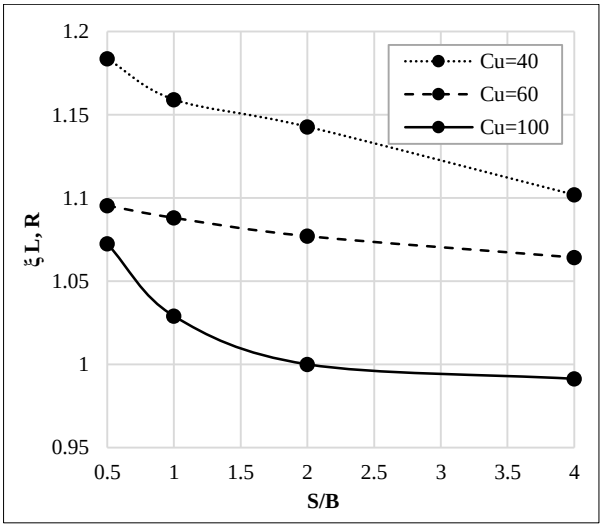

(d)

Figure 12. Variation of $\xi_{L,R}$ with S/B for different Cu and GWT =0 for (a) Df/B = 0.25, (b) Df/B = 0.5, (c) Df/B=1 and (d) Df/B = 1.5

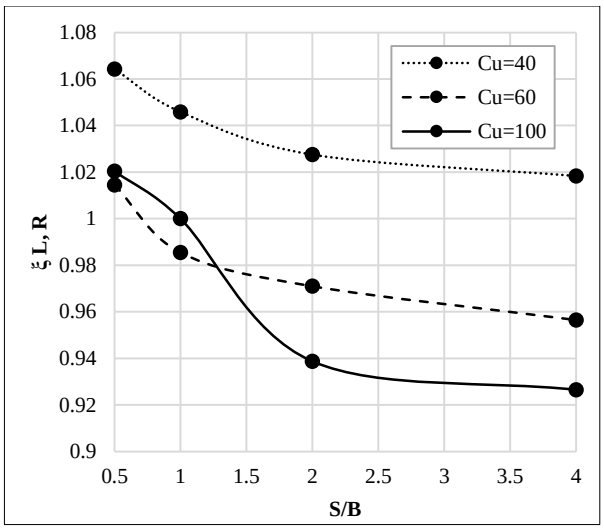

(a)

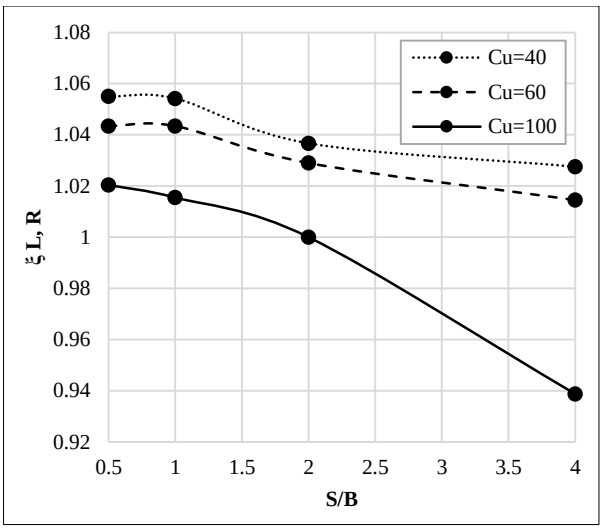

(b)

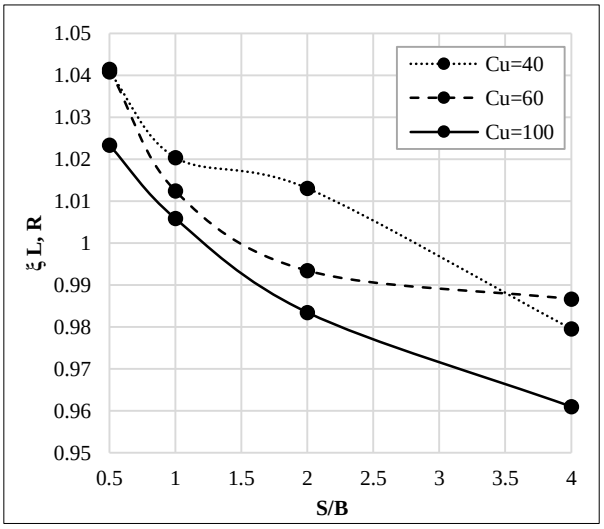

(c)

Figure 13. Variation of $\xi_{L,R}$ with S/B for different Cu and Df/B=0.25 for (a) GWT=0, (b) GWT= 2 m, and (c) GWT = 4 m

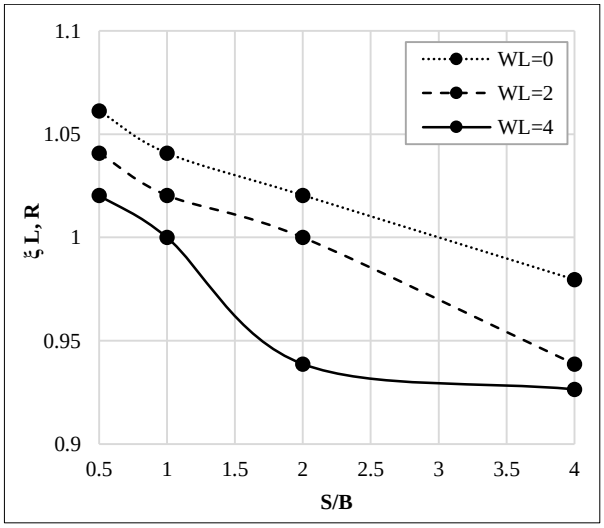

(a)

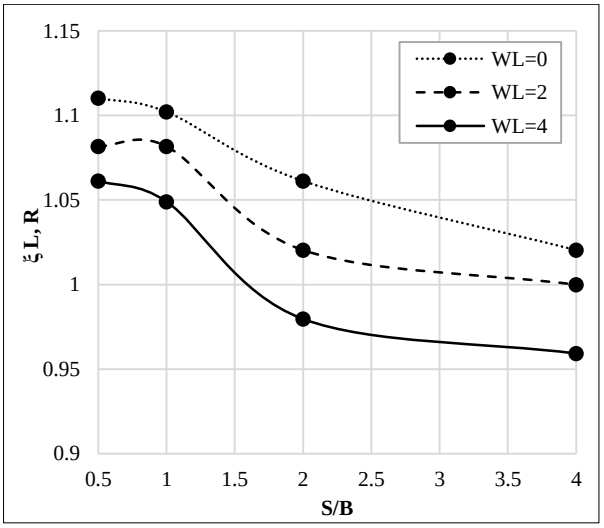

(b)

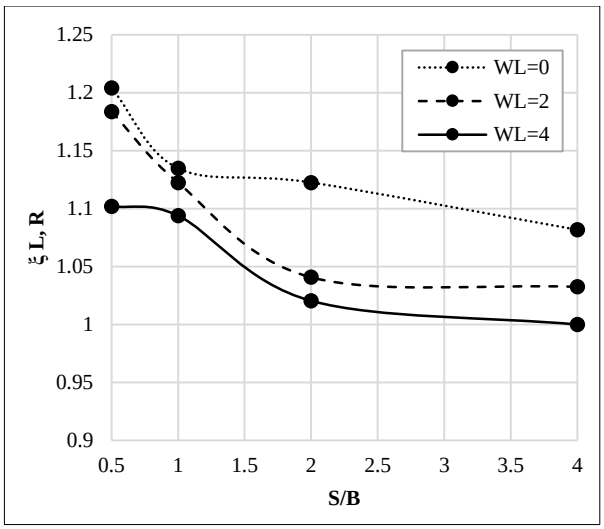

(c)

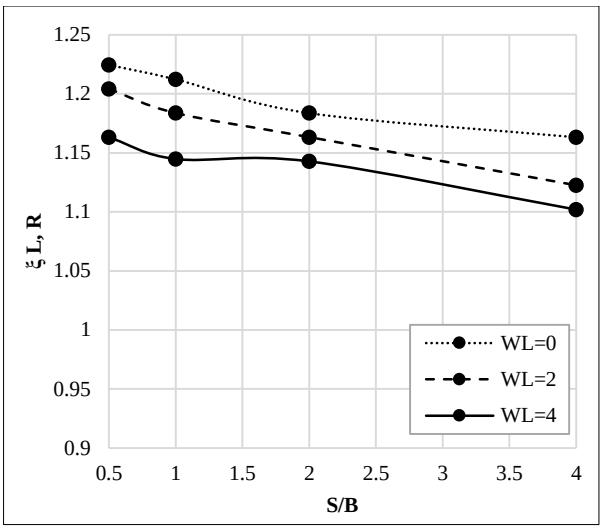

(d)

Figure 14. Variation of ξL, R with S/B for different GWT and Cu= 40 kPa for (a) Df/B = 0.25, (b) Df/B= 0.5, (c) Df/B = 1, and (d) Df/B = 1.5

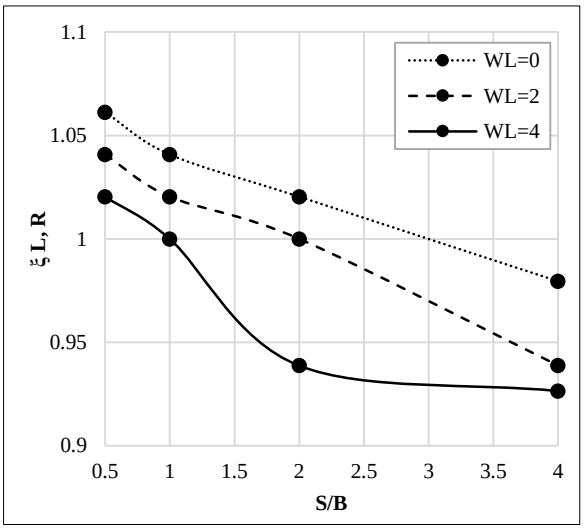

(a)

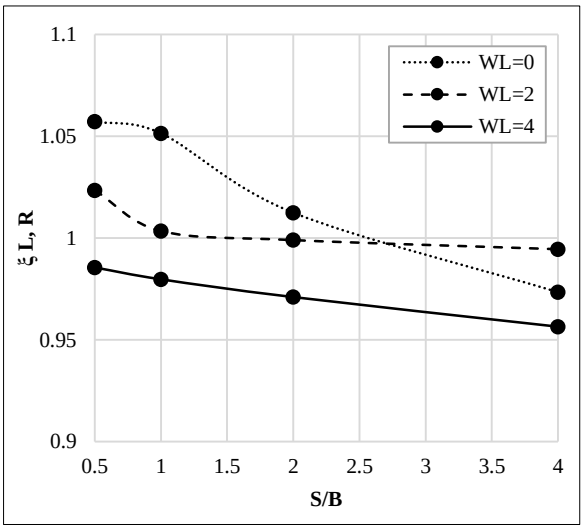

(b)

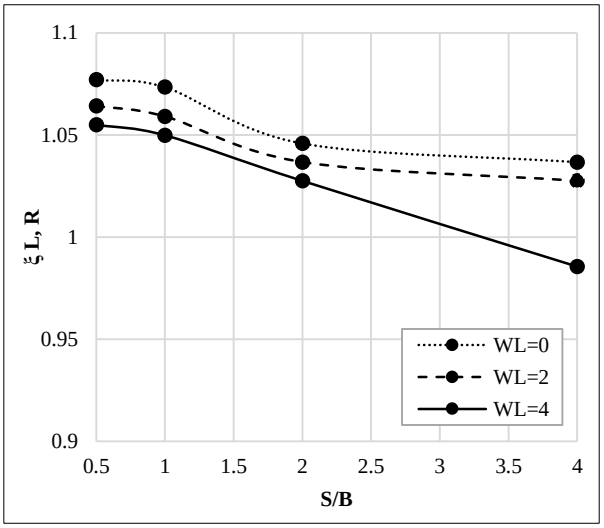

(c)

Figure 15. Variation of $\xi_{L,R}$ with S/B for different GWT and Df/B = 0.25 for (a) Cu= 40 kPa, (b) Cu = 60 kPa, and (c) Cu = 100 kPa

Figure 16 plots the contours of the total settlement of the nearby footings when embedded in clay of cu = 40 kPa with different embedment depths.

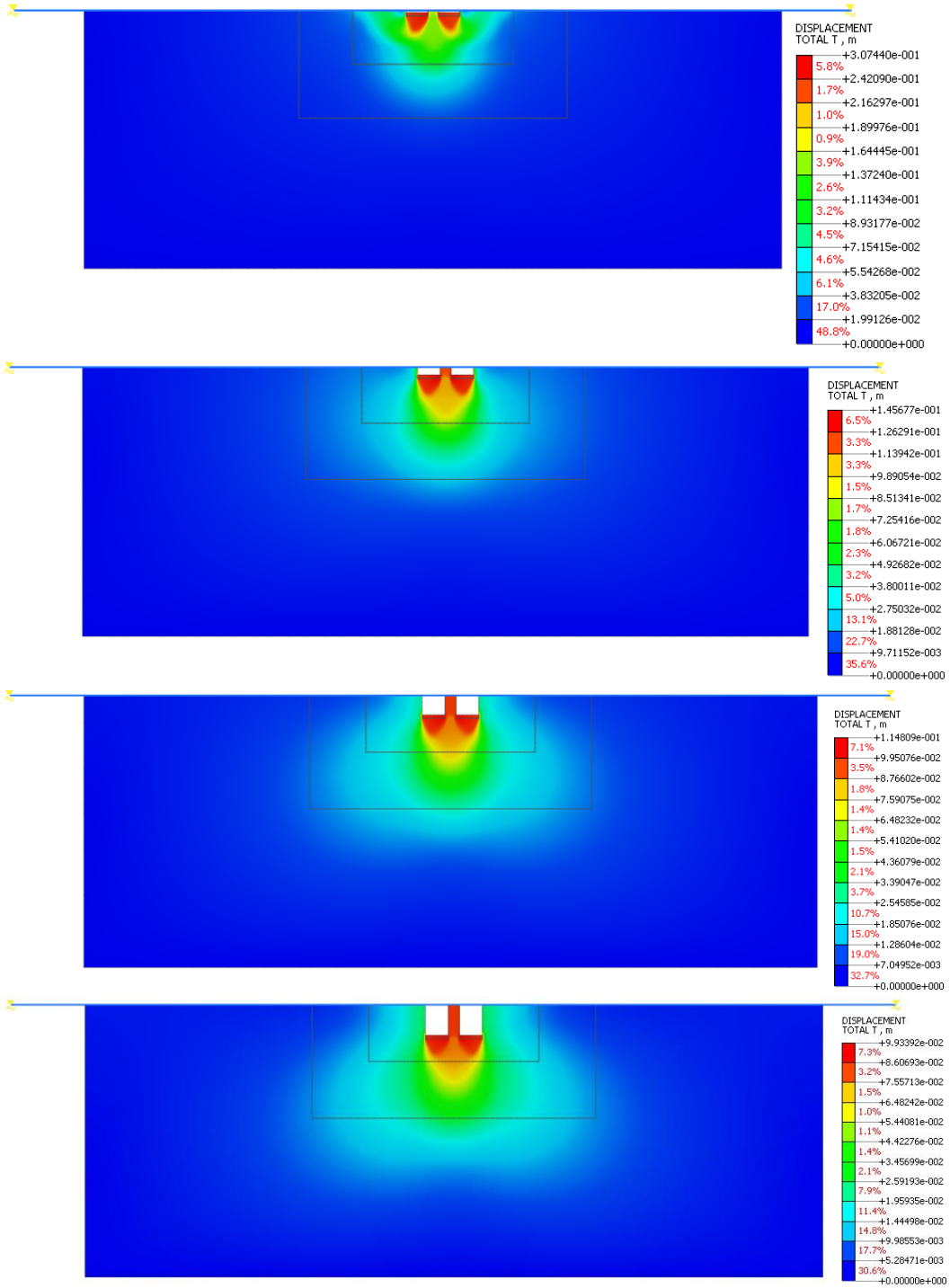

Figure 16. Total-displacement contour plots for Footings of different depths when Cu=40, GWT=0, and S/B=0.5 a) Df/B=0.5, b) Df/B=1, c) Df/B=2, and d) Df/B=3.

When the water table is at the ground surface and S/B = 0.5, it is seen that the footings bearing capacity increases by 20% when compared to an isolated footing. In addition, as can be observed, the shear zone is symmetrical at the footing center and analogous to the failure mechanism suggested by Stuart (1962) [24].

Finally, the proximity of the two embedded footings causes a considerable amount of interference. The bearing capacity is noted to increase with increasing the space between footings until a peak is reached, after which it is observed to decrease with increasing the space between the footings. When the spacing between two footings is from 2-3B, the two shear failure surfaces appear beyond the footing edges in the space between the footings. As a result, the bearing capacity ratio (ξ) decreases. In addition, the soils between footings can carry more loads than the soils under a single footing because they are subject to lateral confining pressures. This explains why the bearing capacity ratio (ξ) increases when two footings are placed next to one another.

5. Conclusions

The effect of two nearby interfering strip footings embedded in saturated cohesive soils was investigated in this paper. A finite element software called Midas GTS Nx has been established for this objective. The clayey soil has been modeled using the Mohr-Coulomb constitutive model, and the footings have been modeled using the linear elastic model. Different factors have been studied, such as the spacing between footings, the depth of footings, the undrained shear strength of the clay, and the groundwater table. The following significant conclusions can be drawn from the results:

- The soil cohesion and the footing depth ratio have a notable influence on the interference of closely spaced footings;
- For all cohesion values, it has been observed that the spacing needed for interference to vanish decreases with an increase in the depth of the footing and water table;
- As the S/B ratio increases, the UBC of interfering footings decreases until it reaches the same value as an isolated footing at greater spacing. The UBC is approximately 10% higher at S/B = 1 compared to the isolated footing;
- The UBC of the interfering footing is observed to drop by 5–10% at S/B = 1 and 2, respectively, while the bearing capacity value of the at-surface footing is still equal to that of the isolated footing, indicating negligible or no influence of interference on the bearing capacity;
- In all cases, the highest values of ξ were obtained when cu = 40 kPa. This indicates that the interaction between footings is greater when the soil is softer.

6. Declarations

6.1. Author Contributions

Conceptualization, M.A. and M.F.; methodology, M.A.; software, M.A.; validation, M.A. and M.F.; formal analysis, M.A.; investigation, M.A. and M.F.; resources, M.A. and M.F.; data curation, M.A. and M. F.; writing—original draft preparation, M.A. and M.F.; writing—review and editing, M.A. and M. F.; supervision, M.F. All authors have read and agreed to the published version of the manuscript.

6.2. Data Availability Statement

The data presented in this study are available on request from the corresponding author.

6.3. Funding

The authors received no financial support for the research, authorship, and/or publication of this article.

6.4. Conflicts of Interest

The authors declare no conflict of interest.

7. References

[1] Das, S., Halder, K., & Chakraborty, D. (2022). Bearing capacity of interfering strip footings on rock mass. Geomechanics and Geoengineering, 17(3), 883–895. doi:10.1080/17486025.2021.1903091.

[2] Shu, S., Gao, Y., Wu, Y., & Ye, Z. (2021). Undrained Bearing Capacity of Two Strip Footings on a Spatially Variable Soil with Linearly Increasing Mean Strength. International Journal of Geomechanics, 21(2). doi:10.1061/(asce)gm.1943-5622.0001904.

[3] Wu, G., Zhao, M., Zhang, R., & Lei, M. (2021). Ultimate Bearing Capacity of Strip Footings on Hoek–Brown Rock Slopes Using Adaptive Finite Element Limit Analysis. Rock Mechanics and Rock Engineering, 54(3), 1621–1628. doi:10.1007/s00603-020-02334-6.

[4] Das, S., & Chakraborty, D. (2022). Effect of Soil and Rock Interface Friction on the Bearing Capacity of Strip Footing Placed on Soil Overlying Hoek–Brown Rock Mass. International Journal of Geomechanics, 22(1), 4021257. doi:10.1061/(asce)gm.1943-5622.0002225.

[5] Das, S., & Chakraborty, D. (2021). Effect of interface adhesion factor on the bearing capacity of strip footing placed on cohesive soil overlying rock mass. Frontiers of Structural and Civil Engineering, 15(6), 1494–1503. doi:10.1007/s11709-021-0768-y.

[6] Acharyya, R., & Dey, A. (2023). Response of Skirted Strip Footing Resting on Layered Granular Soil Using 2-D Plane-Strain Finite Element Modeling. Geotechnical and Geological Engineering. doi:10.1007/s10706-022-02373-6.

[7] Kumar, A., & Saran, S. (2003). Closely spaced footings on geogrid-reinforced sand. Journal of geotechnical and geoenvironmental engineering, 129(7), 660-664. doi:10.1061/(ASCE)1090- 0241(2003)129:7(660).

[8] Ghosh, P., & Kumar, P. (2009). Interference effect of two nearby strip footings on reinforced sand. Contemporary Engineering Sciences, 2(12), 577-592.

[9] Ghosh, P. (2013). Numerical studies on seismic interference of two nearby embedded shallow footings. Disaster Advances, 6(9):19–30.

[10] Nainegali, L. S., Ghosh, P., & Basudhar, P. K. (2013). Interaction of nearby strip footings under inclined loading. Proceedings of the 18th international conference on soil mechanics and geotechnical engineering, 2-6 September, 2013, Paris, France.

[11] Shokoohi, M. A., Veiskarami, M., & Hataf, N. (2019). A Numerical and Analytical Study on the Bearing Capacity of Two Neighboring Shallow Strip Foundations on Sand. Iranian Journal of Science and Technology - Transactions of Civil Engineering, 43(1), 591–602. doi:10.1007/s40996-018-0189-x.

[12] Acharyya, R., Dey, A., & Kumar, B. (2020). Finite element and ANN-based prediction of bearing capacity of square footing resting on the crest of c-φ soil slope. International Journal of Geotechnical Engineering, 14(2), 176–187. doi:10.1080/19386362.2018.1435022.

[13] Anaswara, S., & Shivashankar, R. (2019). A numerical study on interference effects of closely spaced strip footings on soils. International Journal of Civil Engineering and Technology, 10(3).

[14] Boufarh, R., Saadi, D., & Laouar, M. S. (2020). Numerical Investigations on Seismic Bearing Capacity of Interfering Strip Footings. Soils and Rocks, 43(2), 247–259. doi:10.28927/SR.432247.

[15] Meraz, M. M., Mehedi, M. T., & Mim, N. J., (2022). Analytical Prediction of Capacity Variation for Isolated Footings Considering Adjacent Foundations. Proceedings of the 6th International Conference on Civil Engineering for Sustainable Development (ICCESD 2022), 10-12 February, 2022, KUET, Khulna, Bangladesh.

[16] Chen, W. F., & Saleeb, A. F. (1982). Constitutive equations for engineering materials, Vol. 1: Elasticity and modeling. Elsevier, Amsterdam, Netherlands.

[17] Wang, G., & Sitar, N. (2004). Numerical analysis of piles in elasto-plastic soils under axial loading. 17th ASCE Engineering Mechanics Conference, 13-16 June, 2004, University of Delaware, Newark, United States.

[18] Seol, H., Jeong, S., & Kim, Y. (2009). Load transfer analysis of rock-socketed drilled shafts by coupled soil resistance. Computers and Geotechnics, 36(3), 446–453. doi:10.1016/j.compgeo.2008.08.012.

[19] Merifield, R. S., & Nguyen, V. Q. (2006). Two- and three-dimensional bearing-capacity solutions for footings on two-layered clays. Geomechanics and Geoengineering, 1(2), 151–162. doi:10.1080/17486020600632637.

[20] Nguyen, V. Q., & Merifield, R. S. (2011). Undrained bearing capacity of surface footings near slopes. Australian Geomechanics, 46(1), 77.

[21] Lee, J. K., Jeong, S., & Shang, J. Q. (2016). Undrained bearing capacity of ring foundations on two-layered clays. Ocean Engineering, 119, 47–57. doi:10.1016/j.oceaneng.2016.04.019.

[22] Ouahab, M. Y., Mabrouki, A., Frank, R., Mellas, M., & Benmeddour, D. (2020). Undrained Bearing Capacity of Strip Footings Under Inclined Load on Non-homogeneous Clay Underlain by a Rough Rigid Base. Geotechnical and Geological Engineering, 38(2), 1733–1745. doi:10.1007/s10706-019-01127-1.

[23] Ameratunga, J., Sivakugan, N., & Das, B. M. (2016). Correlations of Soil and Rock Properties in Geotechnical Engineering. Developments in Geotechnical Engineering. Springer, New Delhi, India. doi:10.1007/978-81-322-2629-1.

[24] Stuart, J. G. (1962). Interference between foundations, with special reference to surface footings in sand. Geotechnique, 12(1), 15–22. doi:10.1680/geot.1962.12.1.15.